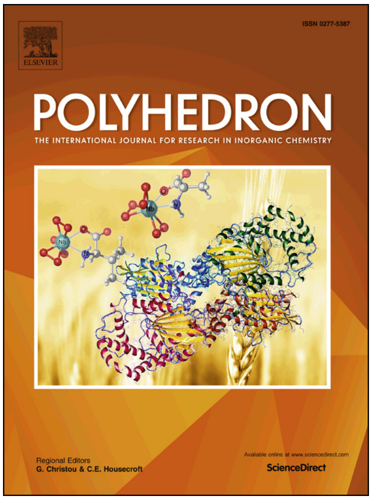

Hexadecachloro-substituted lanthanide(III) phthalocyaninates and their hybrid conjugates with gold nanoparticles: synthesis and optical properties

Elena A. Kuzmina, Tatiana V. Dubinina, Anton V. Zasedatelev, Anton V. Baranikov, Maria I. Makedonskaya, Tolganay B. Egorova, Larisa G. Tomilova

PII: S0277-5387(17)30466-7
DOI: http://dx.doi.org/10.1016/j.poly.2017.06.048
Reference: POLY 12729

To appear in: *Polyhedron*

Received Date: 27 April 2017
Accepted Date: 28 June 2017

Please cite this article as: E.A. Kuzmina, T.V. Dubinina, A.V. Zasedatelev, A.V. Baranikov, M.I. Makedonskaya, T.B. Egorova, L.G. Tomilova, Hexadecachloro-substituted lanthanide(III) phthalocyaninates and their hybrid conjugates with gold nanoparticles: synthesis and optical properties, *Polyhedron* (2017), doi: http://dx.doi.org/10.1016/j.poly.2017.06.048

Hexadecachloro-substituted lanthanide(III) phthalocyaninates and their hybrid conjugates with gold nanoparticles: synthesis and optical properties

Elena A. Kuzmina[a], **Tatiana V. Dubinina**[*a,b], **Anton V. Zasedatelev**[c], **Anton V. Baranikov**[c], **Maria I. Makedonskaya**[a], **Tolganay B. Egorova**[a] **and Larisa G. Tomilova**[a,b]

[a] *Department of Chemistry, M.V. Lomonosov Moscow State University, 1 Leninskie Gory, Moscow, 119991, Russian Federation. Fax: +7 495 939 0290; Tel: +7 495 939 1243; E-mail: dubinina.t.vid@gmail.com.*

[b] *Institute of Physiologically Active Compounds, Russian Academy of Sciences, 1 Severny proezd, Chernogolovka, Moscow Region, 142432, Russian Federation. Fax: +7 496 524 9508; E-mail: tom@org.chem.msu.ru.*

[c] *Skolkovo Institute of Science and Technology, 3 Nobel street, Moscow, 143026, Russian Federation. Fax: +7 495 280 14 81; E-mail: a.zasedatelev@skoltech.ru*

Received date (to be automatically inserted after your manuscript is submitted)

Accepted date (to be automatically inserted after your manuscript is accepted)

ABSTRACT: Novel hexadecachloro-substituted Eu, Er and Lu monophthalocyaninates were prepared via two alternative ways: lanthanide ion templated tetramerization of tetrachlorophthalonitrile and metallation of the corresponding phthalocyanine ligand. Target complexes were identified by mass spectrometry and fourier transform infrared spectroscopy. Aggregation behaviour of these compounds was investigated using UV-vis and fluorescence spectroscopy. Hybrid nanoparticle conjugates composed of the gold cores (20 and 30 nm in diameter) covered by the layers of target phthalocyanines were obtained. The formation of phthalocyanine shell on the surface of nanoparticles and its elemental composition were examined using transmission electron microscopy experiments. Reverse saturable absorption effect was found in solution of the erbium complex utilizing z-scan technique. Furthermore, significant increase in the effect was observed in hybrid nanoparticles due to their plasmonic properties.

KEYWORDS: phthalocyanine, nonlinear optical properties, gold nanoparticles, hybrid conjugates, UV-vis spectroscopy

*Correspondence to: Tatiana V. Dubinina, email: dubinina.t.vid@gmail.com, tel: +7 (495)-9391243, fax: +7 (495)-9390290

INTRODUCTION

Phthalocyanines and their analogues containing electron-withdrawing substituents attract significant research interest due to a wide range of applications. Presence of n-type conductivity [1, 2] allows using of these compounds in organic field-effect transistors and chemical transducers [1]. Furthermore, these complexes can be prospective building blocks for the formation of *push-pull* molecules, revealing nonlinear optical properties [3]. In addition, gas-sensing properties were described for the perchlorinated zinc phthalocyanine [4].

Electron-deficient porphyrazine core can be obtained alternatively either by annelation of electron-deficient heterocycles [5-7] or by introduction of electron-withdrawing substituents [8, 9]. Thanks to high availability of the initial phthalonitriles and capable of further structural modification (e.g. through nucleophilic substitution or cross-coupling reactions) halogen-substituted phthalocyanines are the most attractive derivatives of this type. Typical disadvantages of these compounds resulted from their low solubility: the intrinsic aggregation tendency [1], which usually leads to the broadening and decrease in intensity of the main absorption band (Q-band). Hence, the formation of the high-quality thin films requires application of the relatively expensive vapor deposition technique.

This disadvantage can be overcome employing the synthesis of phthalocyanine complexes with the lanthanide ions. The presence of axial ligands and high coordination ability of lanthanides improves solubility of the target complexes.

Recently, we demonstrated, that it is possible to form hybrid gold nanoparticles covered by tetra-*tert*-butylphthalocyaninato aluminum chloride through axial ligand exchange reaction at the aluminum center of the phthalocyanine [10]. Further growth of phthalocyanine shell is associated with π-πstacking interactions between the phthalocyanine ligands. Great enhancement of the molar absorption coefficient caused by intense plasmonic near field acting on the phthalocyanine shell was established [10]. Present study further extends this work dealing with the synthesis and investigation of optical properties of hexadecachloro-substituted phthalocyaninates of lanthanides and hybrid Au nanoparticles covered by these complexes. Thanks to their tendency to form the most stable single-decker complexes [11-13], the elements of the middle (Eu) and end of lanthanide series (Er and Lu) were chosen as central ions.

MATERIAL AND METHODS

All reactions were monitored by thin-layer chromatography (TLC) and UV-vis until complete disappearance of the starting reagents unless otherwise specified. TLC was performed using Merck Aluminium Oxide F_{254} neutral flexible plates. Electronic absorption (UV/Vis) spectra were recorded on a ThermoSpectronic Helios-α spectrophotometer using quartz cells (1×1 cm). Matrix-assisted laser desorption/ionization time-of-flight (MALDI TOF) mass spectra were taken on a VISION-2000 mass spectrometer with 2,5-dihydroxybenzoic acid (DHB) as the matrix. High-resolution MALDI mass spectra were registered on a Bruker ULTRAFLEX II TOF/TOF instrument with DHB as the matrix. The salts, $Mg(OAc)_2 \cdot 4H_2O$, $Eu(OAc)_3 \cdot 3H_2O$, $Er(OAc)_3 \cdot 4H_2O$, $Lu(OAc)_3 \cdot 4H_2O$ were dried at 70°C for 3 h immediately before use. Tetrachlorophthalonitrile (98%, Sigma-Aldrich), gold nanoparticles 20 nm diameter (stabilized suspension in citrate buffer, $c=7.2\times10^{11}$ particles/mL, Aldrich) and gold nanoparticles 30 nm diameter (stabilized suspension in citrate buffer, $c=1.8\times10^{11}$ particles/mL, Aldrich) were used as received.

The fluorescence spectra were recorded on a Cary Eclipse spectrometer in quartz cells (1×1 cm). Spectral resolution: $\Delta\lambda = 1.5$ nm.

FTIR spectra were measured using IR 200 Thermonicolet spectrometer. Spectral resolution: $\Delta\lambda = 4$ cm^{-1}.

Z-scan measurements were carried out using optical parametric amplifier (Coherent OPerA SOLO) pumped by high energy Ti:sapphire regenerative amplifier system (Coherent Libra-HE) providing TEM00 beam with the emission wavelength of 570 nm. Pulse duration and repetition rate were 100 fs and 100 Hz respectively. The beam was tightly focused by 100 mm focal-length lens providing up to 55 GW/cm^2 peak intensity in the focus. Energy of pulses were in a range from 68 to 75 nJ. All measurements were done in THF solution at room temperature using a 3 mm quartz cuvette.

Synthesis

(a) Approach with tetrachlorophthalonitrile

Preparation of 1,2,3,4,8,9,10,11,15,16,17,18,22,23,24,25-hexadecachlorophthalocyaninato europium acetate 1a: Tetrachlorophthalonitrile (213.0 mg, 0.80 mmol), $Eu(OAc)_3 \cdot 3H_2O$ (76.4 mg, 0.20 mmol) and 1,8-diazabicyclo[5.4.0]undec-7-ene (119 μL, 0.80 mmol) were stirred in 3 mL of boiling isoamil alcohol for 4 h (TLC-control: SiO_2, F_{254}, toluene). The reaction mixture was cooled to room temperature and a $MeOH:H_2O$ (4:1 V/V) mixture was added. The precipitate was filtered and washed with a $MeOH:H_2O$ (4:1 V/V) mixture and dried at 70°C to give compound **1a** (110.8 mg, 44%). UV-vis (THF): λ_{max} (nm) (I/I_{max}) 378 (0.56); 644 (0.35); 696 (1.00). IR (vaseline oil): ν (cm^{-1}) 1050 - 1095 (st C-Cl); 1549 - 1580 (γ pyrrole); 1325 – 1418 (C-O); 1549 – 1614 (C=O). MS (MALDI-TOF): m/z 1180 [M-OAc-Cl]; 1216 [M-OAc]; 1267 [M]; 1362 [M-OAc+DHB]; 1517 [M-OAc+2DHB]. MS (MALDI-TOF/TOF): m/z Found: [M] 1267.4602; molecular formula $C_{34}H_3Cl_{16}EuN_8O_2$ requires [M] 1267.4608.

Preparation of 1,2,3,4,8,9,10,11,15,16,17,18,22,23,24,25-hexadecachlorophthalocyaninato erbium acetate 1b: Tetrachlorophthalonitrile (213.0 mg, 0.80 mmol), $Er(OAc)_3 \cdot 4H_2O$ (83.0 mg, 0.20 mmol) and 1,8-

diazabicyclo[5.4.0]undec-7-ene (119 µL, 0.80 mmol) were stirred in 3 mL of boiling isoamil alcohol for 4 h (TLC-control: SiO_2, F_{254}, toluene). The reaction mixture was cooled to room temperature and a MeOH:H_2O (4:1 V/V) mixture was added. The precipitate was filtered and washed with a MeOH:H_2O (4:1 V/V) mixture and dried at 70°C to give compound **1b** (164.2 mg, 64%). UV-vis (THF): λ_{max} (nm) (I/I_{max}) 361 (0.61); 639 (0.37); 696 (1.00). IR (vaseline oil): ν (cm^{-1}) 1026-1095 (st C-Cl); 1556 (γ pyrrole); 1377 (C-O); 1556 (C=O). MS (MALDI-TOF): m/z 1194 [M-OAc-Cl]; 1212 [M-OAc-Cl+H_2O]; 1229 [M-OAc]; 1247 [M-OAc+H_2O]; 1346 [M-OAc-Cl+DHB]. MS (MALDI-TOF/TOF): m/z Found: [M-OAc] 1229.4486; molecular formula $C_{32}Cl_{16}ErN_8$ requires [M-OAc] 1229.4447.

Preparation of 1,2,3,4,8,9,10,11,15,16,17,18,22,23,24,25-hexadecachlorophthalocyaninato lutetium acetate 1c: Tetrachlorophthalonitrile (213.0 mg, 0.80 mmol), $Lu(OAc)_3 \cdot 4H_2O$ (85.6 mg, 0.20 mmol) and 1,8-diazabicyclo[5.4.0]undec-7-ene (119 µL, 0.80 mmol) were stirred in 3 mL of boiling isoamil alcohol for 4 h (TLC-control: SiO_2, F_{254}, toluene). The reaction mixture was cooled to room temperature and a MeOH:H_2O (4:1 V/V) mixture was added. The precipitate was filtered and washed with a MeOH:H_2O (4:1 V/V) mixture and dried at 70°C to give compound **1c** (202.0 mg, 78%). UV-vis (THF): λ_{max} (nm) (I/I_{max}) 363 (0.68); 642 (0.33); 699 (1.00). IR (vaseline oil): ν (cm^{-1}) 1091 (st C-Cl); 1554 (γ pyrrole); 1377 (C-O); 1554 (C=O). MS (MALDI-TOF): m/z 1444 [M+DHB]; 1502 [M-OAc-Cl+2DHB]; 1536 [M-OAc+2DHB]; 1597 [M+2DHB]; 1655 [M-Cl+3DHB]; 1692 [M-OAc+3DHB]. MS (MALDI-TOF/TOF): m/z Found: [M-OAc+2DHB] 1536.5028; molecular formula $C_{46}H_{10}Cl_{16}LuN_8O_8$ requires [M-OAc+2DHB] 1536.5046.

(b) Approach with hexadecachlorophthalocyanine

Preparation of 1,2,3,4,8,9,10,11,15,16,17,18,22,23,24,25-hexadecachlorophthalocyaninato magnesium 2: Tetrachlorophthalonitrile (426.0 mg, 1.60 mmol), $Mg(OAc)_2 \cdot 4H_2O$ (172.0 mg, 0.40 mmol) and 1,8-diazabicyclo[5.4.0]undec-7-ene (238 µL, 1.60 mmol) were stirred in 6 mL of boiling isoamil alcohol for 4 h (TLC-control: SiO_2, F_{254}, toluene). The reaction mixture was cooled to room temperature and a MeOH:H_2O (4:1 V/V) mixture was added. The precipitate was filtered and washed with a MeOH:H_2O (4:1 V/V) mixture and dried at 70°C to give compound 2 (321.0 mg, 74%). UV-vis (THF): λ_{max} (nm) (I/I_{max}) 365 (0.51); 646 (0.45); 695 (1.00). IR (vaseline oil): ν (cm^{-1}) 1051 - 1101 (st C-Cl); 1556 (γ pyrrole). MS (MALDI-TOF): m/z 1009 [M-2Cl]; 1027 [M-2Cl+H_2O]; 1045 [M-Cl]; 1063 [M-Cl+H_2O]; 1081 [M+H]. MS (MALDI-TOF/TOF): m/z Found: [M+H] 1080.5202; molecular formula $C_{32}HCl_{16}MgN_8$ requires [M+H] 1080.5191.

Preparation of 1,2,3,4,8,9,10,11,15,16,17,18,22,23,24,25-hexadecachlorophthalocyanine 3: The magnesium complex **2** (216.0 mg, 0.20 mmol) was dissolved in concentrated sulphuric acid (10 mL). This solution was poured into the ice. A green precipitate formed at the same time. This precipitate was filtered and washed with water until the neutral pH and MeOH to give **3** (186.0 mg, 87%). UV-vis (THF): λ_{max} (nm) (I/I_{max}) 358 (0.76); 659 (1.00); 697 (0.95). IR (vaseline oil): ν (cm^{-1}) 1039 - 1105 (st C-Cl); 1564 (γ pyrrole); 3300 (st NH). MS (MALDI-TOF): m/z 995

[M-2Cl]; 1012 [M-2Cl+H_2O]; 1030 [M-Cl]; 1048 [M-Cl+H_2O]; 1058 [M+H]. MS (MALDI-TOF/TOF): m/z Found: [M+H] 1058.5468; molecular formula $C_{32}H_3Cl_{16}N_8$ requires [M+H] 1058.5497.

Preparation of 1,2,3,4,8,9,10,11,15,16,17,18,22,23,24,25-hexadecachlorophthalocyaninato europium acetate 1a: A mixture of ligand **3** (164.5 mg, 0.15 mmol) and $Eu(OAc)_3·3H_2O$ (57.3 mg, 0.15 mmol) was refluxed in 3 mL of 1,2-dichlorobenzene (o-DCB) in the presence of 1,8-diazabicyclo[5.4.0]undec-7-ene (37 µL, 0.25 mmol) for 4 h (TLC-control: SiO_2, F_{254}, toluene). The reaction mixture was cooled to room temperature and a MeOH:H_2O (4:1 V/V) mixture was added. The precipitate was filtered and washed with a MeOH:H_2O (4:1 V/V) mixture and dried at 70°C to give compound **1a** (155.0 mg, 81%). The characteristics were identical with those obtained by method (a).

Preparation of 1,2,3,4,8,9,10,11,15,16,17,18,22,23,24,25-hexadecachlorophthalocyaninato erbium acetate 1b: Ligand **3** (78 mg, 0.070 mmol), $Er(OAc)_3·4H_2O$ (29 mg, 0.076 mmol) and 1,8-diazabicyclo[5.4.0]undec-7-ene (18 µL, 0.12 mmol) were stirred in 3 mL of boiling o-DCB for 4 h (TLC-control: SiO_2, F_{254}, toluene). The reaction mixture was cooled to room temperature and a MeOH:H_2O (4:1 V/V) mixture was added. The precipitate was filtered and washed with a MeOH:H_2O (4:1 V/V) mixture and dried at 70°C to give compound **1b** (61 mg, 68%). The characteristics were identical with those obtained by method (a).

Preparation of 1,2,3,4,8,9,10,11,15,16,17,18,22,23,24,25-hexadecachlorophthalocyaninato lutetium acetate 1c: Ligand **3** (80 mg, 0.075 mmol), $Lu(OAc)_3·4H_2O$ (32 mg, 0.075 mmol) and 1,8-diazabicyclo[5.4.0]undec-7-ene (18 µL, 0.12 mmol) were stirred in 3 mL of boiling o-DCB for 4 h (TLC-control: SiO_2, F_{254}, toluene). The reaction mixture was cooled to room temperature and a MeOH:H_2O (4:1 V/V) mixture was added. The precipitate was filtered and washed with a MeOH:H_2O (4:1 V/V) mixture and dried at 70°C to give compound **1c** (77.5 mg, 80%). The characteristics were identical with those obtained by method (a).

Preparation of phthalocyanines 1a-c - gold nanoparticles hybrids. General procedure: The synthesis of hybrids based on gold nanoparticles with a diameter of 20 and 30 nm was carried out by mixing the solutions of gold nanoparticles (1 vol part) in water and a solution of the phthalocyanine in THF ($C=10^{-4}$ M, 9 vol parts). The resulting mixture was kept at room temperature for 2 h.

RESULTS AND DISCUSSION

Synthesis and identification

There are two general synthetic approaches to the lanthanide monophthalocyanine compounds [13]. According to the template method, complexes are obtained starting from corresponding phthalonitriles [14]. The main disadvantage of this approach is of oligomeric and polymeric derivatives of the starting nitrile. Within the second approach the target lanthanide phthalocyaninates are synthesized from the corresponding phthalocyanine ligands [11, 15]. The drawback of this method is the presence of two additional stages: preliminary formation of the magnesium complex and its demetallation.

In the present work both synthetic approaches to phthalocyanine complexes of lanthanides were implemented for their qualitative comparison (Scheme 1).

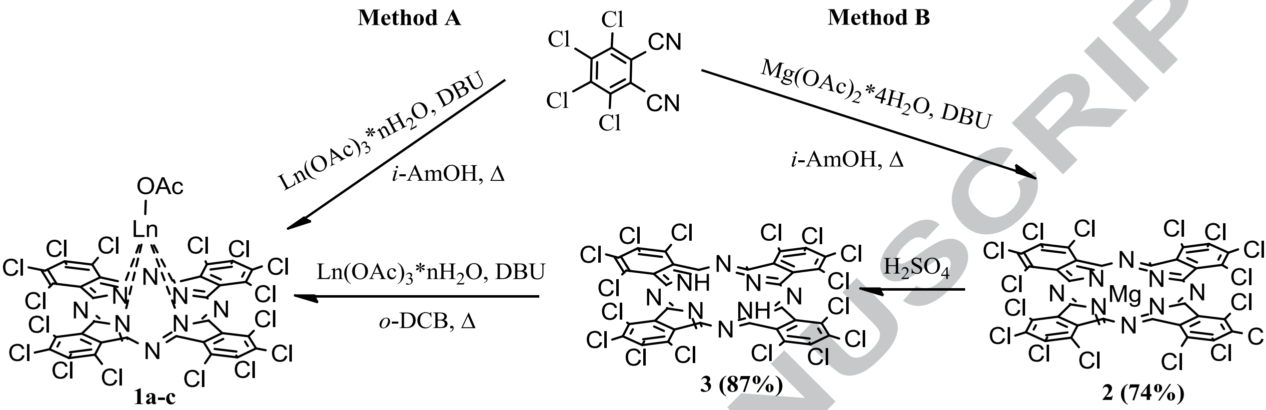

Method A:
1a: Ln=Eu (44%),
1b: Ln=Er (64%),
1c: Ln=Lu (78%)

Method B (yields of the complexes 1 at the final stage):
1a: Ln = Eu (81%),
1b: Ln = Er (68%),
1c: Ln = Lu (80%)

Scheme 1. Synthesis of phthalocyanine complexes **1a-c**.

Template assembly of the compounds **1a–c** (Method A) was performed in boiling isoamyl alcohol. Selectivity of the monophthalocyanine formation was provided by 1,8-diazabicyclo[5.4.0]undec-7-ene (DBU), coordination of which to the lanthanide central ion results in steric hindrance and prevents undesirable formation of the sandwich-type complexes [16]. Due to the possibility of nucleophilic substitution typical for the electron-deficient systems, the use of DBU as a base is preferred rather than employement of alkoxide ions [17]. Decrease of the yields going from lutetium (**1c**) to europium (**1a**) complex can be explained by increase of the Ln^{3+} ionic radius, which is obviously not favorable for template macrocyclization due to steric reasons.

According to the second approach (Scheme 1, Method B) preliminarily formed magnesium complex **2** was demetallated by concentrated sulfuric acid to give ligand **3**. The lanthanide single-deckers **1a–c** were obtained in boiling o-DCB using DBU as a base, by analogy with the previously described procedure [11, 18]. The selective formation of monophthalocyanine complexes **1** was observed without any traces of the double-decker complexes. The total yield of europium complex **1a** (52%) is higher than the yield, which was obtained within the method A (Scheme 1). However, in the case of compounds **1b** and **1c** the first approach turned to be more effective.

All the compounds obtained were characterized by MALDI TOF and high resolution MALDI TOF/TOF mass spectrometry. The high resolution spectra of the target heavy molecular weight lanthanide monophthalocyanines demonstrate good agreement between the observed and calculated mass patterns (see Experimental part). Molecular ions were observed for complexes **1a**, **2** and **3**. The additional fragmentation of peripheral chlorine atoms and axial acetate groups was found. Besides that, the formation of conjugates with the matrix (DHB) under lazer ionization was observed. This phenomenon can be explained by high mobility of axial ions in lanthanide monophthalocyaninates, which can be perfectly applied to obtain heteroleptic complexes [12, 19]. As an example, the mass spectra of the compounds **1a-c** are shown in Fig. 1.

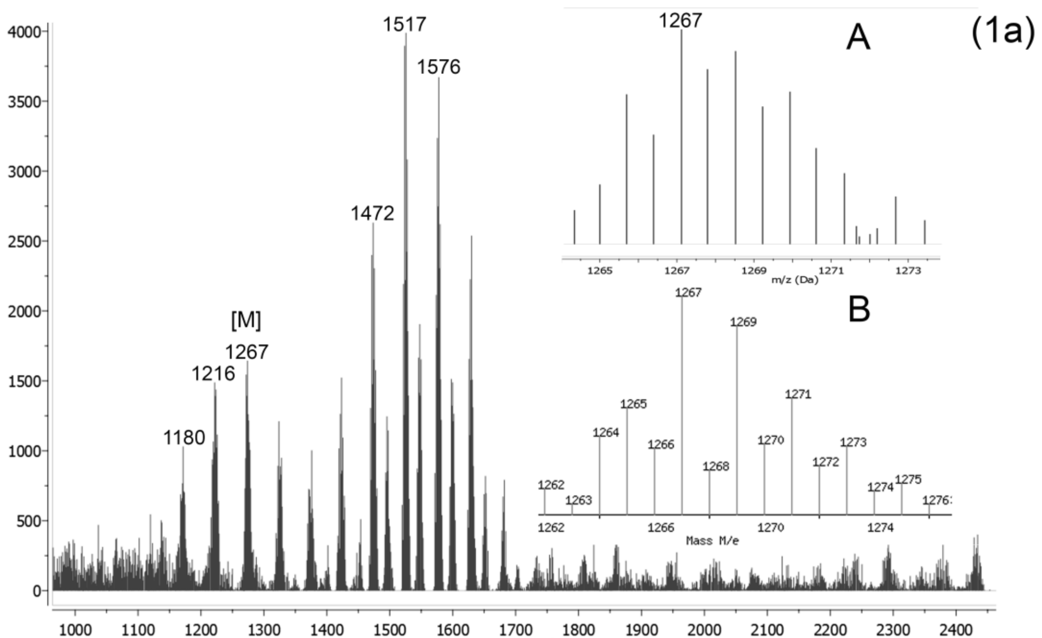
(1a)
A
B
[M]
1180
1216
1267
1472
1517
1576
m/z (Da)
Mass M/e
m/z (Da)

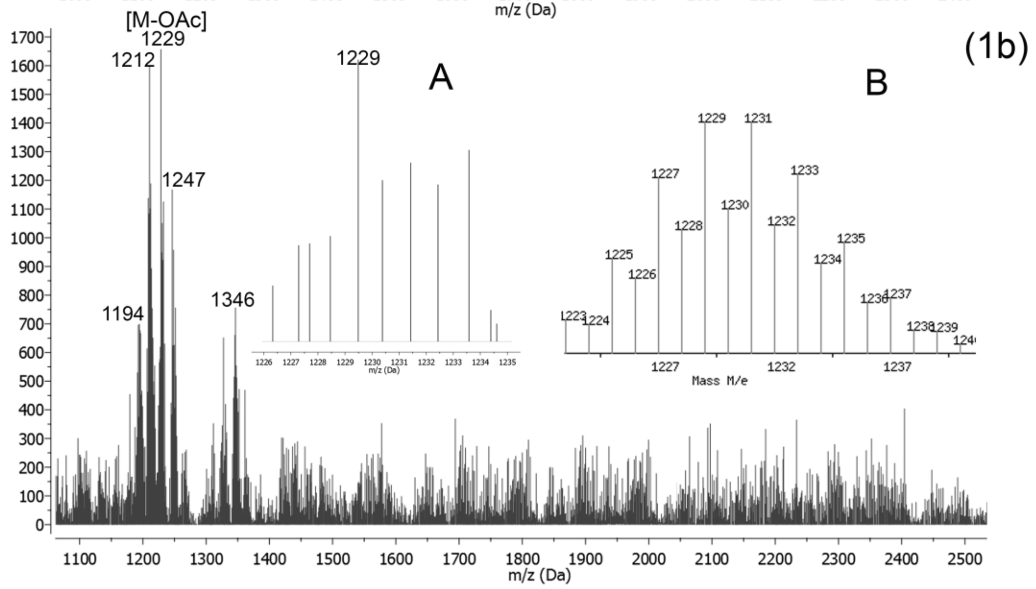
(1b)
A
B
[M-OAc]
1212
1229
1247
1194
1346
m/z (Da)
Mass M/e
m/z (Da)

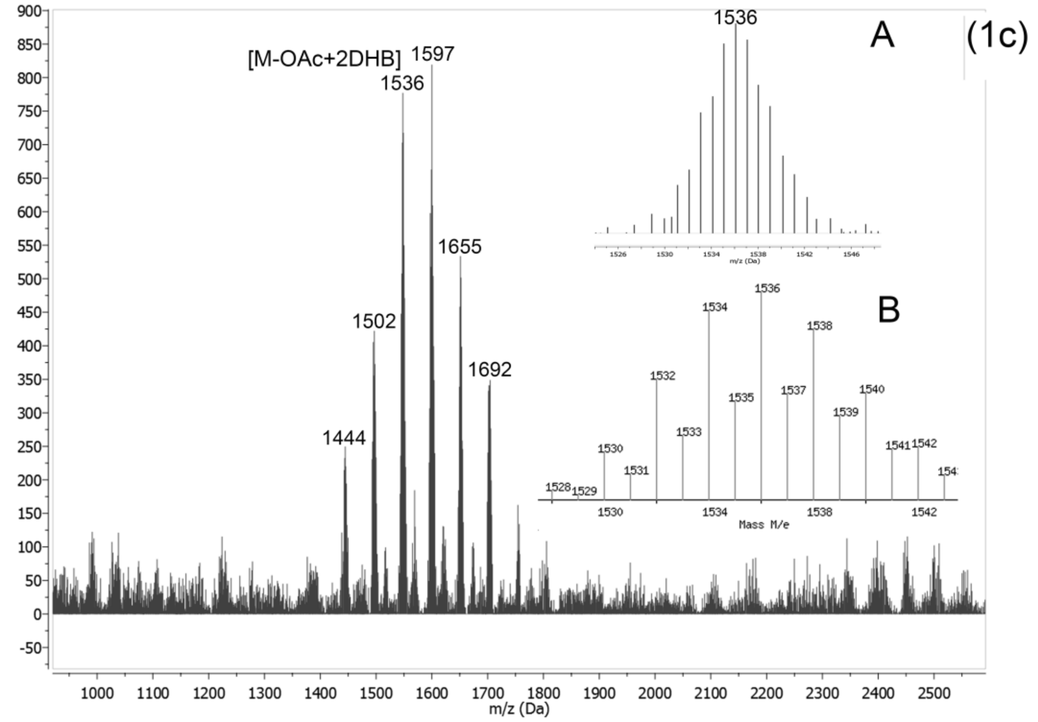
(1c)
A
B
[M-OAc+2DHB]
1536
1597
1655
1502
1692
1444
m/z (Da)
Mass M/e
m/z (Da)

Fig.1. MALDI TOF mass spectra of compounds **1a-c**, isotopic pattern (inset A) and simulated MS pattern (inset B).

FTIR spectra for all target complexes were recorded in vaseline oil. Stretching vibrations of C-Cl bonds were observed in the region of 1026-1105 cm^{-1}. Skeletal vibrations of pyrrol fragments occupy the region from 1549 to 1580 cm^{-1}. In the case of complexes of lanthanide complexes **1a–c** the bands at 1325-1418 cm^{-1} and at 1549-1614 cm^{-1} were assigned to C-O and C=O vibrations respectively.

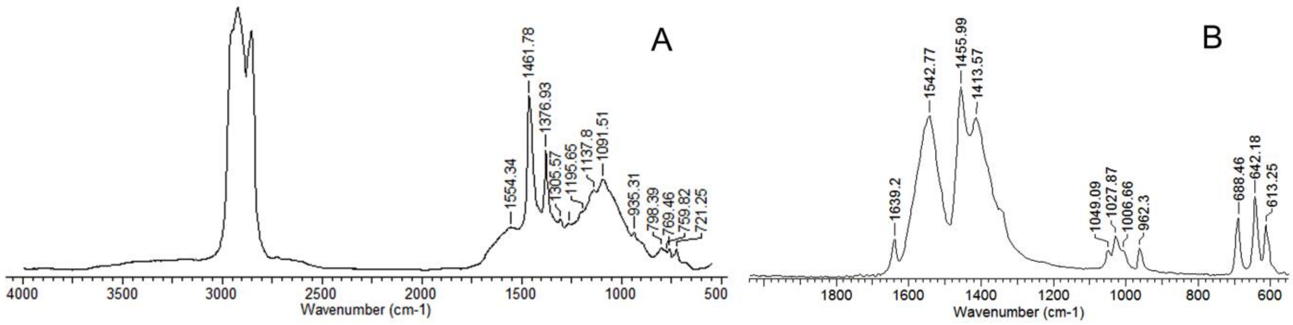

Fig.2. FTIR spectra of lutetium phthalocyaninate **1c** in vaseline oil (A) and lutetium (III) acetate in ZnSe (B).

Notably, the same values were observed for acetates in literature [20] and for the salts used herein. For instance, the spectra of the lutetium complex **1c** and lutetium (III) acetate are shown in Fig. 2.

UV-vis and fluorescence spectroscopy

In the UV-vis spectra of lanthanide phthalocyaninates **1a–c** the type of central ion does not affect the position of the Q-band (Fig. 3).

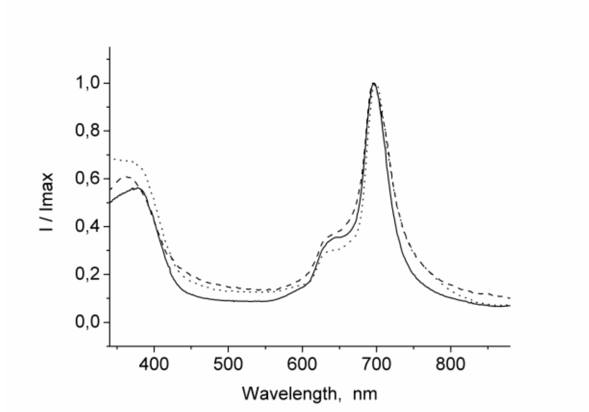

Fig.3. UV-vis spectra of europium **1a** (solid line), erbium **1b** (dashed line) and lutetium **1c** (dotted line) complexes in THF.

For complexes **1** and **2** low resolution of the Q-band vibrational satellites and their increased intensity comparing to the Q-band was observed. The strongest aggregation picture was observed for magnesium complex **2**, which does not contain axial ligand. The aggregation behaviour of complexes **1** and **2** can be explained by the intermolecular interactions between the electron-deficient periphery and the electron-releasing porphyrazine core of the neighboring molecules.

In order to prove this hypothesis fluorescence and excitation spectra were measured for complex **2** (Fig. 4). The Stokes shift of the Q-band is 12 nm. This value is 3 times higher, than Stokes shift in pyrazinoporphyrazines, which were described by us earlier [6].

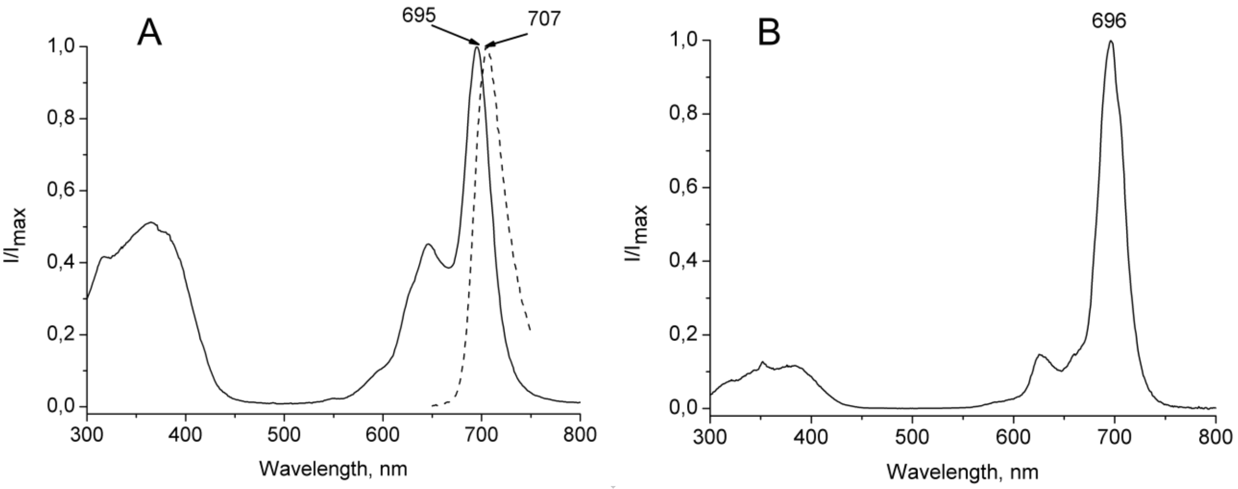

Fig.4. UV-vis (solid line) and fluorescence (dashed line) spectra (λ_{ex} = 380 nm) of **2** in THF (A). Excitation spectrum (λ_{em} = 707 nm) of **2** in THF (B).

In contrast to absorption spectra, Q band vibrational satellites are well-resolved in the excitation spectra and their intensity is lower, than one for absorption spectra. This follows from the fact that the excitation spectra correspond to the shape of nonaggregated complexes.

Identification and optical properties of hybrids

Hybrids of Au nanoparticles and phthalocyanine complexes **1a-c** were prepared in THF solutions. In visible range two main absorption bands were observed: in 520-540 nm region, which can be refered to the absorption band of Au nanoparticles, and near 700 nm, which can be refered to the Q-band of the phthalocyanine part of hybrids (Table 1).

Table 1. Positions of the main absorption bands of hybrid nanoparticles in visible region.

Hybrid	λ(nm)
1a+Au (20 nm)	526; 699
1a+Au (30 nm)	527; 706
1b+Au (20 nm)	527; 697
1b+Au (30 nm)	534;705
1c+Au (20 nm)	527; 702
1c+Au (30 nm)	531; 703

In comparison with pure complexes **1a-c** Q-bands of the hybrids are bathochromically shifted up to 705 and 706 nm in the case of complexes **1a** and **1b**, respectively (Table 1, Fig. 5).

Notheworthy, the most bathochromic shift was found for hybrids with Au (30 nm). In the case of hybrids with Au (20 nm) Q-band possesses a smaller red-shift (1-3 nm). According to the literature data, similar bathochromic shift was observed in the case of Au nanoparticles covered by phthalocyaninato indium chloride [21].

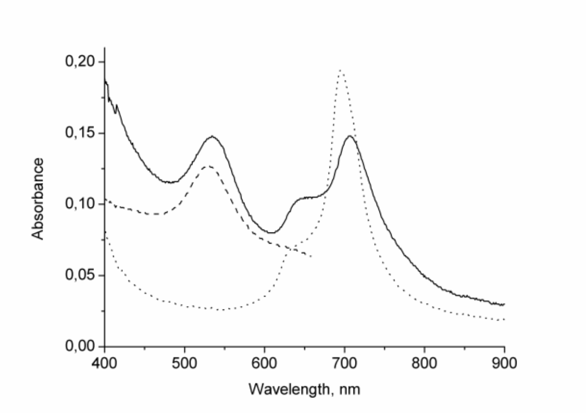

Fig.5. UV-vis spectra of hybrid **1b**+Au (30 nm) (solid line), Au (30 nm) (dashed line) and complex **1b** (dotted line) in THF.

By the analogy with our previous investigation [10], considering the mechanism of the hybrid conjugates formation, we suggest that axial ligand exchange reaction at the lanthanide center of the phthalocyanine (acetate to the anion of citrate OH group) can be considered as the most probable route.

TEM images show the formation of phthalocyanine shell on the surface of gold (Fig. 6). Elemental composition correlates well with the proposed structure and shows the presence of Cl and Eu elements from phthalocyanine and Au - from nanoparticles.

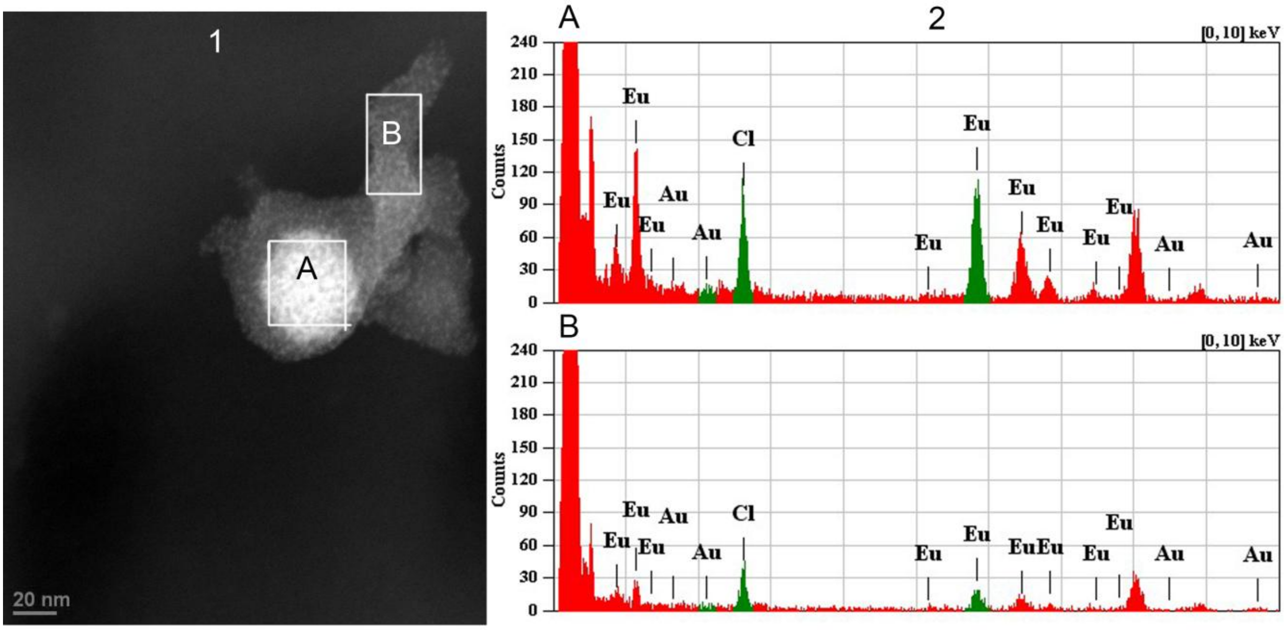

Fig.6. TEM image of hybrid **1a**+Au (20 nm) (1) and elemental composition of the marked regions A and B (2).

According to the TEM data, phthalocyanine shell is not homogeneous, its size occupies the range of 4-14 nm. This probably resulted from the aggregation of phthalocyanine molecules on the surface of gold nanoparticles.

Nonlinear optical (NLO) properties of the samples were studied in accordance with well-known single-beam Z-scan technique first reported by Sheik-Bahae et al [22].

Herein we examined NLO properties of the samples based on **1b** compound conjugated with 20 nm and 30 nm gold nanoparticles with the following concentrations: $1.2 \cdot 10^{-10}$ and $3.0 \cdot 10^{-11}$ M. Open-aperture z-scan data are represented in Fig. 7. In order to extract nonlinear absorption coefficient we fit the result by well-established equation based on the solution of nonlinear wave equation in the paraxial approximation for Gaussian beam [23].

$$T(z) = \sum_{m=0}^{\infty} \frac{(-\beta I_{00} L_{eff})^m}{\left(1 + \left(\frac{z}{z_R}\right)^2\right)^m (m+1)^{\frac{3}{2}}}$$

where β – the nonlinear absorption coefficient, I_{00} – on-axis intensity in focus (*z=0, r=0, t=0*), $L_{eff} = (1 - e^{-\alpha_0 L})/\alpha_0$ – effective thickness of sample, α_0 – the linear absorption coefficeint, z_R - Rayleigh range.

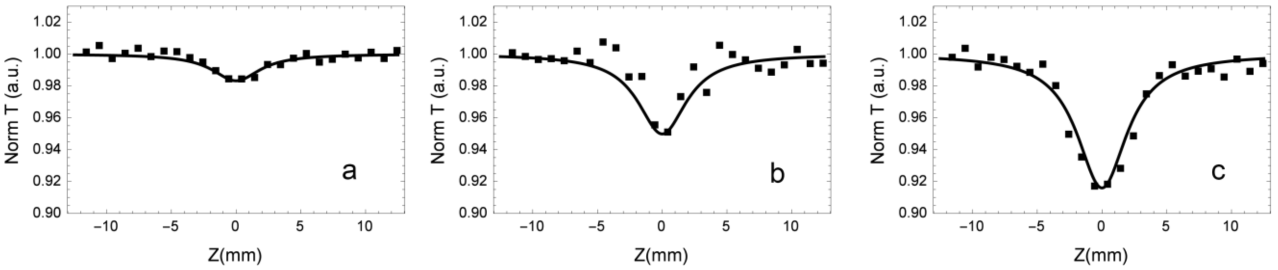

Fig.7 Open-aperture Z-scan curves of compound **1b** – a, compound **1b** + Au (20 nm) – b, compound **1b** + Au (30 nm) – c in THF solution.

Reverse saturable absorption (RSA) effect which was found out in the experiment is not a surprising result for phthalocyanines since the wavelength of excitation lies in transparent region of compound **1b** (Fig.1b). Indeed, in that case the absorption cross-section of $S_0 \rightarrow S_1$ singlet-singlet transition appears to be less than the excited state absorption cross-section of $S_1 \rightarrow S_N$ singlet-singlet transition (Fig. 8). Taking into acount typical values of lifetime in the 1st excited single state for the most of the phthalocyanine compounds (~5 ns) as well as ultrashort pulse duration (100 fs) we can neglect occupancy of the triplet states.

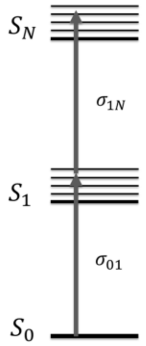

Fig.8 Scheme of optical transitions induced by the nonresonant excitation. S_0 – ground state (singlet), S_1 – 1st excited singlet state, S_N – Nth excited singlet state.

Typically gold nanoparticles demonstate strong saturable absorption effect caused by hot electrons and localized surface plasmon resonance (LSPR) [24]. Open-aperture Z-scan curves for the bare nanoparticles reveal saturable absorption effect explicilty (Fig. 9). Applying analytical model mentioned above the nonlinear coefficients β were found to be equal to $-3\cdot10^{-12}$ cm/W and $-7\cdot10^{-12}$ cm/W for 20 and 30 nm gold nanoparticles respectively. Since the compound **1b** and gold particles exhibit oposite sign nonlinearities having nearly the same amplitudes, their linear superposition should result in decrease of total effect. Nevertheless, one can clearly see pronounced RSA effect for hybrid nanoparticles (Fig. 7b,c). This indicates dominant role of the phthalocyanine nonlinearity in the overall response of the hybrid sample enhanced by gold nanoparticles.

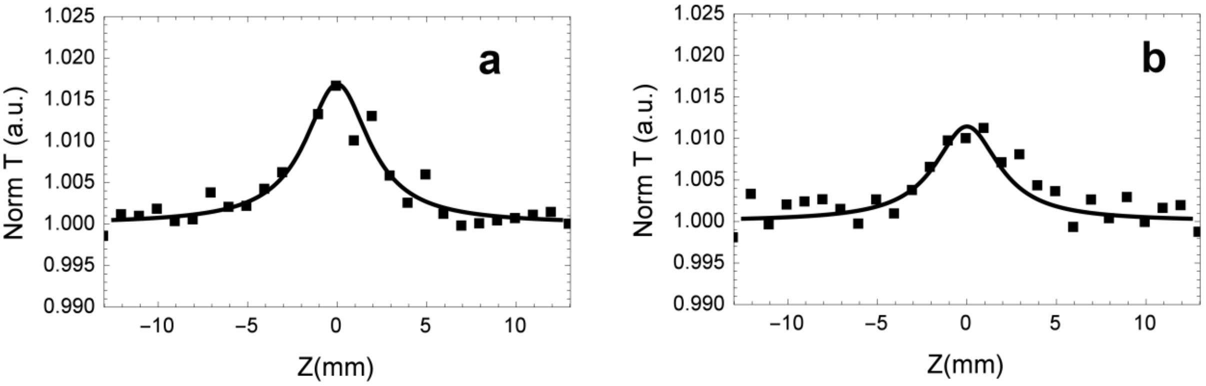

Fig.9 Open-aperture Z-scan curves of 20 nm (a) and 30 nm (b) gold nanoparticles in THF solution.

We found β being much higher for hybrid nanoparticles based on 20 nm ($11\cdot10^{-12}$ cm/W) and 30 nm ($18\cdot10^{-12}$ cm/W) gold cores than β of pure compound **1b** without gold ($3.2\cdot10^{-12}$ cm/W). It should be noted that in the case of resonant excitation of hybrid nanoparticles based on gold cores and subphthalocyanine compounds [25] significant enhancement of nonlinearity was found as well. Hereby we first demonstrate increase in nonlinear absorption, which results in RSA effect utilizing nonresonant excitation. Considerable enhancement in nonlinear absorption for hybrid nanoparticles presumably relates to high local E-field on the nanoparticle surface which is provided by LSPR. In the previous study we demonstrated substantial increase in linear absorption of phthalocyanines attached to gold nanoparticles [10] due to local field factor (LFF). But surface-averaged LFF strongly depends on the particle’s size. In accordance with theory 30 nm particle provides an average field, which is higher than in the case of 20 nm gold. In the present research, we observe the highest nonlinear absorption coefficient for hybrid nanoparticles with the largest gold core that points to the same tendency which was found earlier for the linear absorption.

CONCLUSIONS

Novel hexadecachloro-substituted lanthanide monophthalocyaninates were obtained using template synthesis and reaction of metallation of phthalocyanine ligand (two-stage method). It was observed, that the yields of erbium and lutetium complexes were higher in the template approach. However, the total yield of europium complex is higher in the case of the two-stage method. Target and intermidiate compounds were identified by MALDI TOF mass spectrometry, IR and UV-vis spectroscopy revealing their tendency to aggregation. UV-vis spectrum of the nonaggregated complex was registered as the excitation spectrum. Hybrids of Au nanoparticles (20nm and 30nm) covered by hexadecachloro-substituted lanthanide monophthalocyaninates were prepared. The formation of hybrid nanoparticles was proven by TEM and UV-vis spectroscopy methods. Elemental composition correlates well with proposed structure of the conjugates. Considerable enhancement in nonlinear absorption was observed for hybrid nanoparticles. The highest nonlinear absorption coefficient was found for hybrid particles based on Au (30 nm). This phenomenon can be explained by increase of the local field factor along with increasing the nanoparticle size.

Acknowledgements

We are grateful to the Russian Scientific Fund (Grant 17-13-01197) for main support of this research. The part of this work devoted to the investigated of plasmonic properties was supported by the Russian Foundation for Basic Research (Grant Nos. 16-33-60005, and 16-07-00961) and Council under the President of the Russian Federation for State Support of Young Scientists and Leading Scientific Schools (Grant MD-2991.2017.3). Transmission electron microscopy experiments were realized using the equipment of CKP "Nanochemistry and nanomaterials", which was purchased using the financial resources of the Development Program of M.V. Lomonosov Moscow State University. The authors acknowledge collaboration with Prof Pavlos Lagoudakis, director of the Hybrid Photonics Laboratories at the Skolkovo Institute of Science and Technology, for supporting this work by contributing the z-scan measurements.

REFERENCES

[1] Y. Chen, D. Li, N. Yuan, J. Gao, R. Gu, G. Lu and M. Bouvet, Journal of Materials Chemistry 22 (2012) 22142.

[2] D. Schlettwein, D. Woehrle, E. Karmann and U. Melville, Chemistry of Materials 6 (1994) 3.

[3] G. de la Torre, P. Vázquez, F. Agulló-López and T. Torres, Chemical Reviews 104 (2004) 3723.

[4] Y. Shi, T. Lei, Z. Li, D. Xiu, W. Zhao, Q. Feng and L. Wang, Journal of Semiconductors 30 (2009) 034009.

[5] M. P. Donzello, C. Ercolani, V. Novakova, P. Zimcik and P. A. Stuzhin, Coordination Chemistry Reviews 309 (2016) 107.

[6] A. D. Kosov, T. V. Dubinina, M. Y. Seliverstov, L. G. Tomilova and N. S. Zefirov, Macroheterocycles 9 (2016) 201.

[7] M. Hamdoush, S. S. Ivanova, O. I. Koifman, M. Kos'kina, G. L. Pakhomov and P. A. Stuzhin, Inorganica Chimica Acta 444 (2016) 81.

[8] S. Eu, T. Katoh, T. Umeyama, Y. Matano and H. Imahori, Dalton Transactions (2008) 5476.

[9] K. R. Venugopala Reddy, J. Keshavayya, B. E. Kumara Swamy, M. N. K. Harish, H. R. Mallikarjuna and B. S. Sherigara, Dyes and Pigments 80 (2009) 1.

[10] A. V. Zasedatelev, T. V. Dubinina, D. M. Krichevsky, V. I. Krasovskii, V. Y. Gak, V. E. Pushkarev, L. G. Tomilova and A. A. Chistyakov, The Journal of Physical Chemistry C 120 (2016) 1816.

[11] T. V. Dubinina, K. V. Paramonova, S. A. Trashin, N. E. Borisova, L. G. Tomilova and N. S. Zefirov, Dalton Transactions 43 (2014) 2799.

[12] V. E. Pushkarev, L. G. Tomilova and V. N. Nemykin, Coordination Chemistry Reviews 319 (2016) 110.

[13] V. E. Pushkarev, L. G. Tomilova and V. T. Yu, Russian Chemical Reviews 77 (2008) 875.

[14] A. V. Ivanov, P. A. Svinareva, I. V. Zhukov, L. G. Tomilova and N. S. Zefirov, Russian Chemical Bulletin 52 (2003) 1562.

[15] S. Bo, D. Tang, X. Liu and Z. Zhen, Dyes and Pigments 76 (2008) 35.

[16] Y. G. Gorbunova, L. A. Lapkina, A. G. Martynov, I. V. Biryukova and A. Y. Tsivadze, Russian Journal of Coordination Chemistry 30 (2004) 245.

[17] E. H. Mørkved, N. K. Afseth and H. Kjøsen, Journal of Porphyrins and Phthalocyanines 10 (2006) 1301.

[18] V. E. Pushkarev, M. O. Breusova, E. V. Shulishov and Y. V. Tomilov, Russian Chemical Bulletin 54 (2005) 2087.

[19] T. V. Dubinina, A. D. Kosov, E. F. Petrusevich, S. S. Maklakov, N. E. Borisova, L. G. Tomilova and N. S. Zefirov, Dalton Transactions 44 (2015) 7973.

[20] K. Nakamoto, Infrared and Raman Spectra of Inorganic and Coordination Compounds, 1986, p.484

[21] N. Nwaji, D. O. Oluwole, J. Mack, M. Louzada, S. Khene, J. Britton and T. Nyokong, Dyes and Pigments 140 (2017) 417.

[22] M. Sheik-Bahae, A. Said and E. Van Stryland, Optics letters 14 (1989) 955.

[23] M. Sheik-Bahae, A. A. Said, T. H. Wei, D. J. Hagan and E. W. V. Stryland, IEEE Journal of Quantum Electronics 26 (1990) 760.

[24] Y. Guillet, M. Rashidi-Huyeh and B. Palpant, Physical Review B 79 (2009) 045410.

[25] A. Zasedatelev, T. Dubinina, V. Krasovskii, O. Suprunova, L. Tomilova and A. Chistyakov, Journal of Physics: Conference Series 643 (2015) 012049.

- Effective approach to perchlorinated lanthanide phthalocyaninates was developed.
- Hybrids composed of the gold cores covered by phthalocyanines were obtained.
- Aggregation behaviour was investigated using UV-vis and fluorescence spectroscopy.
- Enhancement in nonlinear absorption was observed for hybrid nanoparticles.
- The highest nonlinear absorption coefficient was found for hybrids with Au 30 nm.

Novel perchlorinated Eu, Er and Lu monophthalocyaninates were prepared. Hybrid nanoparticle conjugates composed of the gold cores (20 and 30 nm in diameter) covered by the layers of target phthalocyanines were obtained. Considerable enhancement in nonlinear absorption was observed for hybrid nanoparticles.